



Synthesis and crystal structure of K_2NiF_4 -type novel $Gd_{1+x}Ca_{1-x}AlO_{4-x}N_x$ oxynitrides



Yuji Masubuchi*, Tomoyuki Hata, Teruki Motohashi, Shinichi Kikkawa

Faculty of Engineering, Hokkaido University, N13 W8, Kita-ku, Sapporo, Hokkaido 060-8628, Japan

ARTICLE INFO

Article history:

Received 28 June 2013

Received in revised form 2 August 2013

Accepted 24 August 2013

Available online 31 August 2013

Keywords:

Inorganic materials

Rare earth alloys and compounds

Solid state reactions

Crystal structure

Synchrotron radiation

X-ray diffraction

ABSTRACT

Novel gadolinium calcium aluminum oxynitrides, $Gd_{1+x}Ca_{1-x}AlO_{4-x}N_x$, were prepared in $x = 0.15$ – 0.25 by the solid state reaction of a nitrogen-rich mixture with AlN as an aluminum source; the mixture was sintered twice at $1500\text{ }^\circ\text{C}$ for 5 h under 0.5 MPa of nitrogen gas. Shift in the optical absorption edge was observed in their diffuse reflectance spectra from 4.46 eV for the oxide ($x = 0$) to 2.94 eV for the oxynitride at $x = 0.2$. The crystal structure of $Gd_{1.2}Ca_{0.8}AlO_{3.8}N_{0.2}$ at $x = 0.2$ was refined using a synchrotron X-ray diffraction data as a layered K_2NiF_4 -type structure with the $I4mm$ space group. Longer Al–O/N bond lengths in the oxynitride than those in $GdCaAlO_4$ suggest that the nitride ions are in the apical site of aluminum polyhedron, similar to those in Nd_2AlO_3N .

© 2013 Elsevier B.V. All rights reserved.

1. Introduction

Multinary oxynitride compounds are attracting much attention in applications such as white light emitting diodes (LEDs) [1,2], visible light driven photocatalysts [3,4], inorganic pigments [5,6] and dielectric materials [7–12]. The optical properties of the oxynitrides in the UV–vis range have been explained by the coexistence of nitride and oxide anions together because of the more covalent nature in nitride ion [13]. Much research on phosphor materials for LED applications has been conducted on silicon oxynitride and aluminosilicon oxynitrides as host materials [14–16]. However, study on (oxy)nitrides of especially aluminum is limited to systems such as AlN:Eu, spinel-type AlON:Mg,Mn, and $BaAl_{11}O_{16}N:Eu$ [17–19]. Magnetoplumbite-type aluminum oxynitride doped with Eu was reported to be a phosphor material to have emission in multiple wavelength [20]. Neutron diffraction study showed that the emission site split because they have a slightly different coordination in the presence of both nitride and oxide ions together [21].

RE_2AlO_3N oxynitride ($RE = La, Nd, Sm$) with K_2NiF_4 -type structure ($n = 1$ in Ruddlesden–Popper phase, $A_{n+1}B_nX_{3n+1}$) has been prepared by firing mixtures of RE_2O_3 and AlN in a small sealed nickel tube at a high temperature ($1350\text{ }^\circ\text{C}$) under N_2 flow [22]. Crystal structure refinement of Nd_2AlO_3N using its neutron diffraction data showed an ordering of nitride and oxide ions in the reduced

symmetry from $I4/mmm$ in K_2NiF_4 to $I4mm$ in Nd_2AlO_3N [23]. The nitride ion is located at an apical site of AlO_5N octahedron. There are two kinds of rare earth sites; Nd1 coordinated with O_8N and Nd2 coordinated with O_5N_4 , as shown in Fig. 1. Sr_2TaO_3N crystallizes in K_2NiF_4 -type structure with $I4/mmm$ space group. Its nitride ions are located at equatorial sites of TaO_4N_2 octahedron, and there is only one crystallographic Sr site, (4e) [24]. Several kinds of aluminum oxides $AEREAlO_4$ ($AE = Ca, Sr, RE = La, Nd, Sm, Gd$) have also been reported to crystallize in $I4/mmm$ space group [25–27].

The oxynitride was found out in a preparation using a nickel tube. An alternative preparation method, such as the carbon reduction nitridation method, has been applied to prepare Nd_2AlO_3N and Sm_2AlO_3N [28]. La_2AlO_3N and Gd_2AlO_3N can be utilized as a multi-color emitting phosphor host material when they will be doped with divalent Eu. They have two crystallographic rare earth sites induced by O/N ordering, as mentioned above for Nd_2AlO_3N . Photoluminescence property of divalent Eu can be controlled by changing its coordination environment such as coordination number and O/N ratio.

In our preliminary study, La_2AlO_3N has been tried to obtain in solid state reaction but there was no appearance of the oxynitride in the products prepared using a similar method described in this paper. Gd_2AlO_3N has not yet been obtained in the carbon reduction nitridation [28], because the size of the Gd^{3+} ion is not compatible with the K_2NiF_4 -type structure. However, the $GdCaAlO_4$ phase is successfully prepared by the simple solid state reaction [29]. The ionic radius of Gd^{3+} in 9 coordination is 0.124 nm, which is smaller

* Corresponding author. Tel./fax: +81 (0)11 706 6742/6740.

E-mail address: yuji-mas@eng.hokudai.ac.jp (Y. Masubuchi).

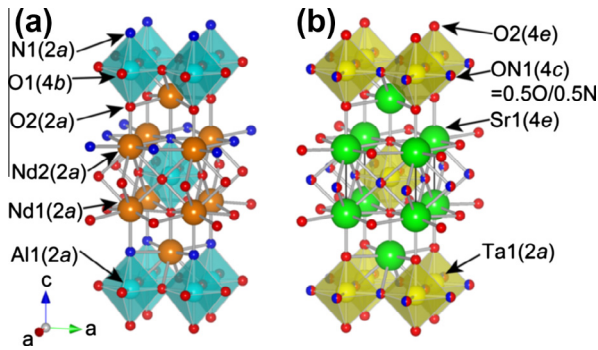


Fig. 1. Crystal structures of K_2NiF_4 -type oxynitrides: (a) Nd_2AlO_3N ($I4mm$) and (b) Sr_2TaO_3N ($I4/mmm$).

than Nd^{3+} (0.130 nm) and Sm^{3+} (0.127 nm); however, the mixing Gd^{3+} with Ca^{2+} (0.132 nm) will increase their average size to stabilize K_2NiF_4 structure [30]. In this study, a series of K_2NiF_4 -type gadolinium calcium aluminum oxynitrides, $Gd_{1+x}Ca_{1-x}AlO_{4-x}N_x$, were prepared by co-substituting Ca^{2+} and O^{2-} in $GdCaAlO_4$ with Gd^{3+} and N^{3-} simultaneously by the solid state reaction. Their crystal structure was investigated by high resolution synchrotron X-ray diffraction analysis.

2. Experimental

Gd_2O_3 (99.9%, Wako Pure Chemicals Co.), $CaCO_3$ (99.9%, Wako Pure Chemicals Co.), $\gamma-Al_2O_3$ (99.95%, Kojundo Chem. Lab. Co.), and AlN (Grade H, Tokuyama Co.) were used as starting materials. Gd_2O_3 was calcined at 1000 °C for 10 h before mixing with other powders. The powders were dry mixed in stoichiometric ratios for $Gd_{1+x}Ca_{1-x}AlO_{4-x}N_x$ with $x = 0-0.3$ in a dry nitrogen atmosphere to avoid hydrolysis of AlN with moisture. The mixed powders were uniaxially pressed at 20 MPa to form 10 mm diameter disks, which were then fired in a gas pressure furnace at 1500 °C for 5 h under a nitrogen pressure of 0.5 MPa. The aluminum source was either AlN only or a mixture of AlN and $\gamma-Al_2O_3$. For AlN only as the aluminum source, the cation composition, i.e., $Gd:Ca:Al = 1 + x:1-x:1$, was maintained; however, the anionic composition was variable during the reaction. A part of AlN was expected to be oxidized during synthesis process. When AlN without $\gamma-Al_2O_3$ was used, the starting mixtures were fired twice with an intermediate grinding and mixing step.

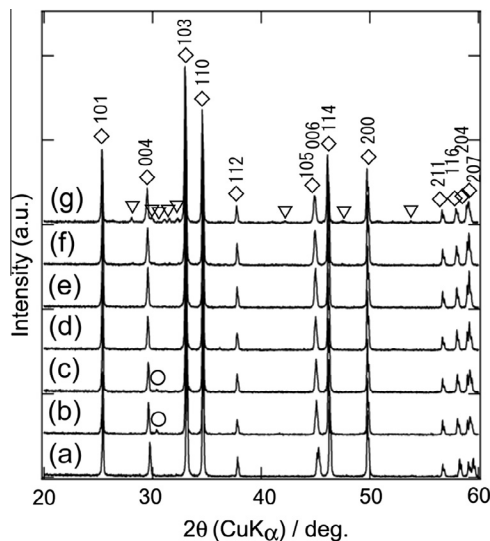


Fig. 2. XRD patterns of products obtained from starting mixtures with AlN only as the aluminum source for $Gd_{1+x}Ca_{1-x}AlO_{4-x}N_x$ at $x =$ (a) 0, (b) 0.05, (c) 0.1, (d) 0.15, (e) 0.20, (f) 0.25, and (g) 0.30. The product obtained for $x = 0$ ($GdCaAlO_4$, (a)) was prepared using $\gamma-Al_2O_3$ as the aluminum source. Diffraction lines marked with diamonds, triangles and circles indicate the K_2NiF_4 -type $Gd_{1+x}Ca_{1-x}AlO_{4-x}N_x$, Gd_2O_3 , and $CaAl_2O_4$ phases, respectively.

The crystalline phases were characterized by powder X-ray diffraction (XRD; Ultima IV, Rigaku) with monochromatized $Cu K\alpha$ radiation. XRD patterns were collected over the 2θ range of 10–120° with a step size of 0.02°. For structural refinement of $Gd_{1+x}Ca_{1-x}AlO_{4-x}N_x$, high resolution synchrotron powder XRD experiments was performed at room temperature using a Debye–Scherrer camera installed at beamline BLO2B2 of the Japan Synchrotron Radiation Institute (SPring-8). The incident beam was monochromatized to 0.035459 nm. The finely ground powder samples were put into a 0.2 mm \varnothing glass capillary. The Rietveld program RIETAN-FP [31] was used for crystal structure refinement. The crystal structures were visualized using the VESTA program [32]. The nitrogen content was measured with an oxygen/nitrogen analyzer (EMGA-620 W, Horiba) using Si_3N_4 as a reference. Diffuse reflectance spectra were measured using a spectrophotometer (V-550, Jasco) in the range of 250–750 nm.

3. Results and discussion

3.1. Preparation of $Gd_{1+x}Ca_{1-x}AlO_{4-x}N_x$ oxynitrides

The products obtained from stoichiometric mixtures using both $\gamma-Al_2O_3$ and AlN as aluminum source were contaminated with Gd_2O_3 . A single phase of $Gd_{1+x}Ca_{1-x}AlO_{4-x}N_x$ with the K_2NiF_4 -type structure was obtained only at $x = 0$, that is $GdCaAlO_4$. Simultaneous substitution of Ca^{2+} and O^{2-} pair with Gd^{3+} and N^{3-} together led to the K_2NiF_4 -type oxynitride products with a small impurity phase of Gd_2O_3 . The amount of the Gd_2O_3 impurity phase increased with an increase in x . Diffraction lines from the (00 l) planes of the K_2NiF_4 -type structure shifted toward a smaller diffraction angle with increasing x . Elongation of the c -axis has been observed similarly from the $CaNdAlO_4$ oxide ($a = 0.36847(3)$ nm and $c = 1.2124(2)$ nm) to Nd_2AlO_3N oxynitride ($a = 0.37046(2)$ nm and $c = 1.25301(13)$ nm) [23,27]. The increase of the lattice parameter c suggests the formation of $Gd_{1+x}Ca_{1-x}AlO_{4-x}N_x$ oxynitride with the K_2NiF_4 -type structure. The appearance of Gd_2O_3 impurity may indicate nitrogen deficiency in $Gd_{1+x}Ca_{1-x}AlO_{4-x}N_x$ due to partial oxidation of AlN during the synthesis.

The K_2NiF_4 -type $Gd_{1+x}Ca_{1-x}AlO_{4-x}N_x$ oxynitride obtained from starting mixtures containing both $\gamma-Al_2O_3$ and AlN was contaminated with the Gd_2O_3 impurity phase losing nitrogen during the reaction. Therefore, AlN only was used as the aluminum source in the starting mixtures to improve the phase purity. Single phase of $Gd_{1+x}Ca_{1-x}AlO_{4-x}N_x$ was obtained between $x = 0.15$ and 0.25 as shown in Fig. 2. AlN was expected to be partially oxidized during the synthesis process. The suitable O/N ratio was attained to form a pure oxynitride phase between $x = 0.15$ and 0.25 in the reaction.

$CaAl_2O_4$ and Gd_2O_3 were observed as secondary phases at $x = 0.1$ and 0.30, respectively. The product obtained at $x = 0.2$ had an expanded c -axis ($a = 0.3658(1)$ nm and $c = 1.2067(5)$ nm) compared to that for $GdCaAlO_4$ ($a = 0.3658(2)$ nm and $c = 1.1994(6)$ nm) at $x = 0$. The nitrogen content of the $x = 0.2$ oxynitride

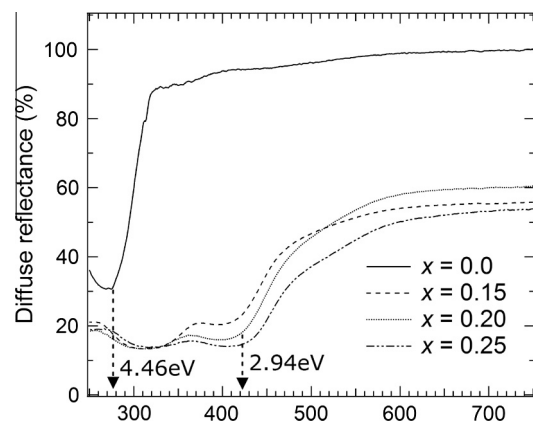


Fig. 3. Diffuse reflectance spectra of $Gd_{1+x}Ca_{1-x}AlO_{4-x}N_x$.

Table 1
Band gap energies and lattice parameters for $Gd_{1-x}Ca_{1-x}AlO_{4-x}N_x$.

| x | Composition | Band gap (eV) | Lattice parameters ^a | |
|------|---|---------------|---------------------------------|-----------|
| | | | a (nm) | c (nm) |
| 0.0 | GdCaAlO ₄ | 4.46 | 0.3658(2) | 1.1994(6) |
| 0.15 | Gd _{1.15} Ca _{0.85} AlO _{3.85} N _{0.15} | 2.96 | 0.3659(3) | 1.2059(9) |
| 0.20 | Gd _{1.2} Ca _{0.8} AlO _{3.8} N _{0.2} | 2.94 | 0.3658(1) | 1.2067(5) |
| 0.25 | Gd _{1.25} Ca _{0.75} AlO _{3.75} N _{0.25} | 2.91 | 0.3658(2) | 1.2072(7) |

^a Lattice parameters were calculated from the laboratory XRD data.

was 1.2(1) wt%, which is comparable with the theoretical nitrogen content of 0.9 wt% within $\pm 3\sigma$. The $x = 0.20$ oxynitride was expected to have an O/N ratio of 3.8/0.2 to maintain the charge neutrality. The lattice expansion may be due to partial substitution of O^{2-} ($r = 0.124$ nm, $c.n. = 4$) by N^{3-} ($r = 0.134$ nm, $c.n. = 4$), although Gd^{3+} ($r = 0.124$ nm, $c.n. = 9$) is smaller than Ca^{2+} ($r = 0.132$ nm, $c.n. = 9$) [30]. Anisotropic expansion along the c -axis implies the ordering of nitride ions in the apical sites of AlO_5N octahedron, similarly to the crystal structure reported for the Nd_2AlO_3N oxynitride with fully ordered nitride ions on the apical site ($2a$), as shown in Fig. 1(a) [23].

The color of the resultant oxynitrides was yellow,¹ while GdCaAlO₄ was white. The absorption edges were at ca. 4.46 eV and 2.94 eV for the oxide ($x = 0$) and oxynitride ($x = 0.2$), respectively, as shown in Fig. 3. The color change occurred with the nitrogen incorporation to form a new valence band at higher energy position than O(2p) orbital level, as reported for many oxynitride pigments [5,6,13]. The edge positions of the oxynitrides obtained at $x = 0.15$ – 0.25 slightly shifted toward longer wavelength along with the nitrogen content, x . The shift in edge positions indicated a decrease in band gap of $Gd_{1-x}Ca_{1-x}AlO_{4-x}N_x$, implying an elevated valence band level as increasing in the nitrogen content. Table 1 summarizes the optical band gap energy and lattice parameters of the oxynitrides. Ordering of the nitride ions in the apical site of Al octahedron induces two kinds of Gd/Ca sites coordinated with N-rich or N-poor anions as shown in Fig. 1(a). Absorption edge positions can be attributed to the N-rich Gd/Ca polyhedron, because of the higher energy level of the nitrogen 2p orbital than that of oxygen. The decrease in band gap energy might be interpreted as nitrogen enrichment in the former Gd/Ca polyhedron. Crystal structure of the oxynitride at $x = 0.20$ is discussed in the next section.

3.2. Crystal structure refinement at the $Gd_{1.2}Ca_{0.8}AlO_{3.8}N_{0.2}$ oxynitride

The crystal structure of $Gd_{1.2}Ca_{0.8}AlO_{3.8}N_{0.2}$ was refined using the high resolution synchrotron XRD pattern in the K_2NiF_4 -type structure with the $I4mm$ space group, starting from the reported crystallographic parameters for Nd_2AlO_3N [23]. The O/N ratios for three anionic sites were fixed at 0.95/0.05, because of their mutually similar X-ray scattering factors. Neutron diffraction has been generally used for analysis of the oxygen and nitrogen distribution in oxynitrides; however, it is not useful for the present products, because the Gd atom has a large neutron absorption cross section. The finally refined parameters from the Rietveld method are summarized in Table 2. Observed, calculated, and difference synchrotron XRD profiles for $Gd_{1.2}Ca_{0.8}AlO_{3.8}N_{0.2}$ are shown in Fig. 4. The refined occupancies for Gd/Ca sites indicate a chemical composition of $Gd_{1.22(1)}Ca_{0.78(1)}AlO_{3.8}N_{0.2}$, which is in agreement with the nominal starting composition of $Gd_{1.2}Ca_{0.8}AlO_{3.8}N_{0.2}$. The bond lengths and the atomic arrangements around Al and Gd/Ca sites are summarized in Table 3 and shown in Fig. 5(a), respectively.

¹ For interpretation of color in Fig. 1, the reader is referred to the web version of this article.

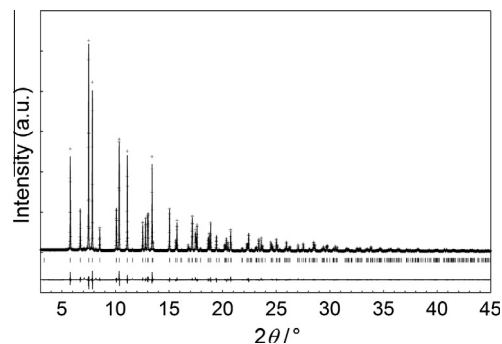


Fig. 4. Observed (+), calculated (solid line) and difference synchrotron XRD profiles for K_2NiF_4 -type $Gd_{1.2}Ca_{0.8}AlO_{3.8}N_{0.2}$. Vertical bars indicate the positions of Bragg reflections.

Table 2
Refined structural parameters of $Gd_{1.2}Ca_{0.8}AlO_{3.8}N_{0.2}$ in K_2NiF_4 -type structure.

| Atom | Site | g | x | y | z | B_{iso} ($\times 10^{-2}$ nm ²) |
|--------|------|------------------------|-----|-----|-----------|--|
| Al | 2a | 1 | 0 | 0 | 0.0118(9) | 0.56(3) |
| Gd/Ca1 | 2a | 0.614/0.386(8) | 0 | 0 | 0.3657(4) | 0.33(6) |
| Gd/Ca2 | 2a | 0.606/0.394(5) | 0 | 0 | 0.6509(4) | 0.35(6) |
| O/N1 | 4b | 0.95/0.05 ^a | 0 | 1/2 | 0.0151(8) | |
| O/N2 | 2a | | 0 | 0 | 0.8329(8) | 0.38(6) ^b |
| O/N3 | 2a | | 0 | 0 | 0.1689(7) | |

$R_{wp} = 5.4\%$, $R_p = 4.1\%$. S.G.: $I4mm$, $a = 0.365850(1)$ nm, $c = 1.206752(8)$ nm.

^a Site occupations, g , for anion sites were fixed as 0.95/0.05N.

^b Isotropic displacement parameters, B_{iso} , for anion sites were analyzed using a constrains: $B(O/N1) = B(O/N2) = B(O/N3)$.

Table 3
Selected bond lengths (nm) in $Gd_{1.2}Ca_{0.8}AlO_{3.8}N_{0.2}$.

| $Gd_{1.2}Ca_{0.8}AlO_{3.8}N_{0.2}$ | S.G.: $I4mm$ | | |
|------------------------------------|--------------|------------|------------|
| Al (2a) | O/N1 (4b) | $\times 4$ | 0.18297(2) |
| | O/N2 (2a) | $\times 1$ | 0.2160(18) |
| | O/N3 (2a) | $\times 1$ | 0.1900(19) |
| Gd/Ca1 (2a) | O/N1 (4b) | $\times 4$ | 0.2568(8) |
| | O/N2 (2a) | $\times 4$ | 0.2617(2) |
| | O/N3 (2a) | $\times 1$ | 0.2375(11) |
| Gd/Ca2 (2a) | O/N1 (4b) | $\times 4$ | 0.2456(8) |
| | O/N2 (2a) | $\times 1$ | 0.2197(11) |
| | O/N3 (2a) | $\times 4$ | 0.2596(2) |

The crystal structure of GdCaAlO₄ reported by Vasylechko, et al. [26] using a powder XRD pattern is also shown in Fig. 5(b). The oxynitride has c -axis much longer than the reported value for GdCaAlO₄ (1.19787 nm), while a -axis is almost similar between the oxynitride and oxide. The elongated c -axis is attributed to longer Al–O/N2 bond length of 0.2160(18) nm in the oxynitride than the corresponding distance of 0.2027 nm for Al–O in the oxide. Similarly elongated bond lengths have been observed for Al–N bond length in Nd_2AlO_3N compared with $NdCaAlO_4$. The nitride ions are located at the apical sites of AlO_5N octahedron in Nd_2AlO_3N [23]. The bond length of Al–N was reported to be 0.1893 nm for $c.n. = 4$ in AlN, which is longer than that of Al–O (0.1710 nm for $c.n. = 4$ in γ - Al_2O_3) [33,34]. The longer bond lengths of Al–O/N2 indicate the preferential occupation of nitride ions on O/N2 sites in the present $Gd_{1.2}Ca_{0.8}AlO_{3.8}N_{0.2}$, as reported in Nd_2AlO_3N [20]. The preferential occupation of nitride ion might elongate the chemical bond between Gd/Ca and O/N2. On the other hand, the refined bond length is 0.2617(2) nm for Gd/Ca1–O/N2 which is comparable to the reported value of 0.2609 nm in the corresponding oxide. Substitution of O^{2-} with N^{3-} can increase the bond length, while smaller Gd^{3+} cation also replaces a part of bigger

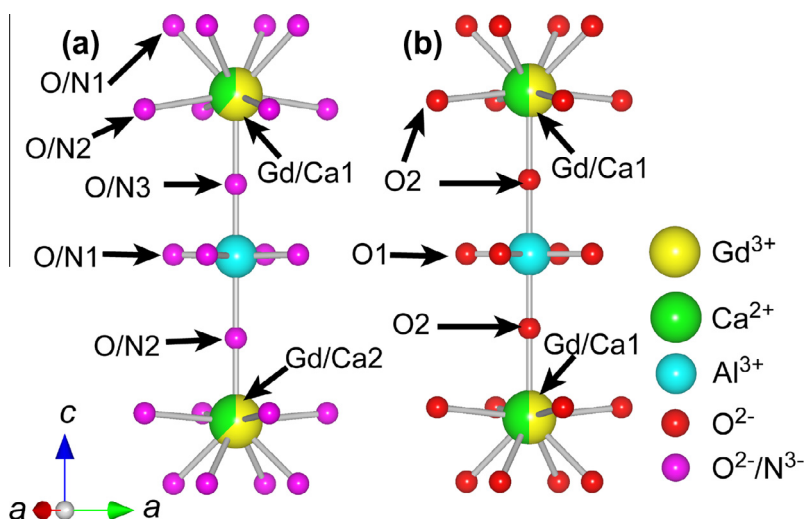


Fig. 5. Atomic arrangement around Al and Gd/Ca sites in (a) $Gd_{1.2}Ca_{0.8}AlO_{3.8}N_{0.2}$ ($I4mm$) and (b) $GdCaAlO_4$ ($I4/mmm$). The schematic structure of $GdCaAlO_4$ was drawn using the reported structural parameters [26].

Ca^{2+} cation in the oxynitride. Therefore the bond length between Gd/Ca and O/N does not change significantly from the oxide to the oxynitride. BVS calculation was performed in the oxynitride. The value is +3.06 for the Al ion and is larger than theoretical value of +, when a random distribution of O/N ions on the anion sites is assumed. The BVS value is improved to be +3.01 in the ordering of the nitride ions only in O/N2 site, supporting the preferential occupation of nitride ions in O/N2 site. Structure refinement in $I4/mmm$ space group showed much less agreement with R_{wp} value of 5.6%. The refined bond length of Al–O/N2 was shorter than that of Al–O in the oxide, although the refined Gd/Ca1–O/N2 bond length was longer than that in the oxide. Both the poor fitting of the oxynitride and the decrease in the Al–O/N2 bond length of $Al(O,N)_6$ octahedron exclude the $I4/mmm$ space group for the structural refinement of the $Gd_{1.2}Ca_{0.8}AlO_{3.8}N_{0.2}$ oxynitride. The present oxynitride crystallizes in $I4mm$ space group having non-equivalent Gd/Ca1 and Gd/Ca2 sites. Preparation and photoluminescence property of Eu doped $Gd_{1+x}Ca_{1-x}AlO_{4-x}N_x$ are currently being investigated.

4. Conclusions

Novel gadolinium calcium aluminum oxynitrides, $Gd_{1+x}Ca_{1-x}AlO_{4-x}N_x$ ($x = 0.15–0.25$), were prepared by the solid state reaction from a nitrogen-rich starting composition. Diffuse reflectance spectra showed the shift in absorption edge from oxide (4.46 eV) to oxynitride at $x = 0.2$ (2.94 eV) due to the nitrogen incorporation. The crystal structure refinement of the $Gd_{1.2}Ca_{0.8}AlO_{3.8}N_{0.2}$ oxynitride using synchrotron XRD showed the elongation of the Al–O/N bond length in aluminum octahedron similar to the Nd_2AlO_3N , indicating that the nitride ions are preferentially in the apical site of the aluminum octahedron in the oxynitride. The preferential occupation of nitride ion on a specific anion site forms two distinct Gd/Ca sites making the oxynitride to future application for a novel multi-color emitting phosphor host material for divalent Eu doping.

References

- [1] R.J. Xie, N. Hirotsaki, K. Sakuma, Y. Yamamoto, M. Mitomo, Appl. Phys. Lett. 84 (2004) 5404–5406.
- [2] T. Suehiro, N. Hirotsaki, R.J. Xie, M. Mitomo, Chem. Mater. 17 (2005) 308–314.
- [3] K. Maeda, K. Domen, J. Phys. Chem. C 111 (2007) 7851–7861.
- [4] K. Maeda, T. Takata, M. Hara, N. Saito, Y. Inoue, H. Kobayashi, K. Domen, J. Am. Chem. Soc. 127 (2005) 8286–8287.
- [5] M. Jansen, H.P. Letschert, Nature 404 (2000) 980–982.
- [6] M. Pérez-Estébanez, R. Pastrana-Fábregas, J. Isasi-Marín, R. Sáez-Puche, J. Mater. Res. 21 (2006) 1427–1433.
- [7] Y.I. Kim, P.M. Woodward, K.Z. Baba-Kishi, C.W. Tai, Chem. Mater. 16 (2004) 1267–1276.
- [8] Y.R. Zhang, T. Motohashi, Y. Masubuchi, S. Kikkawa, J. Ceram. Soc. Jpn. 119 (2011) 581–586.
- [9] Y.R. Zhang, T. Motohashi, Y. Masubuchi, S. Kikkawa, J. Eur. Ceram. Soc. 32 (2012) 1269–1274.
- [10] M. Yang, J. Oro-Sole, J.A. Rodgers, A.B. Jorge, A. Fuentes, J.P. Attfield, Nat. Chem. 3 (2011) 47–52.
- [11] Y. Hinuma, H. Moriwake, Y.R. Zhang, T. Motohashi, S. Kikkawa, I. Tanaka, Chem. Mater. 24 (2012) 4343–4349.
- [12] Y.R. Zhang, Y. Masubuchi, T. Motohashi, S. Kikkawa, K. Hirota, Ceram. Int. 39 (2013) 3377–3380.
- [13] F. Tessier, P. Maillard, F. Chevire, K. Domen, S. Kikkawa, J. Ceram. Soc. Jpn. 117 (2009) 1–5.
- [14] X. Piao, T. Horikawa, H. Hanzawa, K. Machida, Appl. Phys. Lett. 88 (2006) 161908/1–3.
- [15] Y. Masubuchi, M. Yoshikawa, T. Takeda, S. Kikkawa, J. Alloys Comp. 487 (2009) 409–412.
- [16] X.W. Zhu, Y. Masubuchi, T. Motohashi, S. Kikkawa, J. Alloys Comp. 489 (2010) 157–161.
- [17] N. Hirotsaki, R.J. Xie, K. Inoue, T. Sekiguchi, B. Dierre, K. Tamura, Appl. Phys. Lett. 91 (2007). 061101/1–3.
- [18] R.J. Xie, N. Hirotsaki, X.J. Liu, T. Takeda, H.L. Li, Appl. Phys. Lett. 92 (2008). 201905/1–3.
- [19] S.R. Jansen, J.M. Migchels, H.T. Hintzen, R. Metselaar, J. Electrochem. Soc. 146 (1999) 800–806.
- [20] S. Kikkawa, N. Hata, T. Takeda, J. Am. Ceram. Soc. 91 (2008) 924–928.
- [21] Y. Masubuchi, T. Hata, T. Motohashi, S. Kikkawa, J. Solid State Chem. 184 (2011) 2533–2537.
- [22] R. Marchand, C.R. Acad. Sci. Paris 282 (1976) 329–331.
- [23] R. Marchand, R. Pastuszak, Y. Laurent, G. Roult, Rev. Chim. Miner. 19 (1982) 684–689.
- [24] N. Diot, R. Marchand, J. Haines, J.M. LeHger, P. Macaudiere, S. Hull, J. Solid State Chem. 146 (1999) 390–393.
- [25] X.C. Fan, X.M. Chen, X.Q. Liu, Chem. Mater. 20 (2008) 4092–4098.
- [26] L. Vasylychko, N. Kodama, A. Matkovskii, Y. Zhydachevskii, J. Alloys Comp. 300–301 (2000) 475–478.
- [27] R.D. Shannon, R.A. Oswald, J.B. Parise, B.H.T. Chai, P. Byszewski, A. Pajaczowska, R. Sobolewski, J. Solid State Chem. 98 (1992) 90–98.
- [28] F. Chevire, A. Pallu, E. Ray, F. Tessier, J. Alloys Comp. 509 (2011) 5839–5842.
- [29] L. Zhou, J. Shi, M. Gong, J. Rare Earths 24 (2006) 138–142.
- [30] R.D. Shannon, Acta Crystallogr. A 32 (1976) 751–767.
- [31] F. Izumi, K. Momma, Solid State Phenom. 130 (2007) 15–20.
- [32] K. Momma, Fujio Izumi, J. Appl. Crystallogr. 41 (2008) 653–658.
- [33] G.A. Jeffrey, G.S. Parry, R.L. Mozzi, J. Chem. Phys. 25 (1956) 1024–1031.
- [34] E.J.W. Verwey, Z. Kristallogr. 91 (1935) 317–320.